Front. Earth Sci. 2024, 18(2): 384–399
https://doi.org/10.1007/s11707-022-1077-z

RESEARCH ARTICLE

# Control of slope-pattern on the deposition of fan-delta systems: a case study of the Upper Karamay Formation, Junggar Basin

**Mingxuan GAO[1,2], Xinghe YU[1,2], Shunli LI (✉)[1,2], Wenmiao ZHANG[3], Songhao HU[4], Menglu ZHANG[4]**

1 School of Energy Resource, China University of Geosciences, Beijing 100083, China
2 Key laboratory of marine reservoir evolution and hydrocarbon enrichment mechanism (Ministry of Education), China University of Geosciences, Beijing 100083, China
3 College of Geosciences, China University of Petroleum, Beijing 102249, China
4 No.1 Oil Production Plant, Xinjang Oilfield Company, Karamay 834099, China



**Abstract** The Mesozoic fan deltas in the north-west margin of the Junggar Basin, as important petroleum reservoirs, exhibited complex facies change and internal structures with strong heterogeneity which were controlled by the transformation of slope-patterns, bringing great challenges to the study of sedimentary characteristics. The Upper Karamay Formation at north-west margin of the Junggar Basin was the objective in this paper which attempts to clarify the mechanism of sedimentary response and sand-body distribution of fan delta systems under the control of slope-pattern change. Based on a data set of cores, well logs and seismic, two types of slope-pattern were identified in the study area, which include steep-to-gentle in the south and gentle-to-steep in the north. The control of difference slope-patterns on the sand-body distribution was clarified based on the analysis of the sedimentary dynamics, facies characteristics, and depositional evolution of the fan deltas. The study shows that the transport mechanism of sediments on the steep-slope was dominated by debris flows, developing coarse-grained, thick-bedded lobes with poor structural maturity of clasts. On the gentle-slope, the deposition was dominated by hyperconcentrated-traction currents, forming relatively fine-grained, thin-bedded lobes with increased sandy matrix. The sand-bodies show frequent bar-channel transformation and channel down-cutting under the steep slope setting, which exhibit migration of isolated river channels on the gentle slopes. Under the steep-to-gentle pattern, the coase-grained sediments were mainly accumulated at slope toe, generally developed equiaxial lobes. However, the coarse-grained clasts were preserved both at proximal and distal lobes on the gentle-to-steep slopes, showing obvious lateral extension of the fan delta. The slope patterns controlled sedimentary respond rates of the fan deltas during lake level change. By comparing the modern cases of fan systems worldwide, the control of slope patterns on deposition of coarse-grained fans was clarified, providing insight into hydrocarbon exploration on basin margins.

**Keywords** fan delta, slope-pattern, sedimentary characteristics, the Upper Karamay Formation

## 1 Introduction

In recent years, with the continuous improvement of petroleum exploration and development technology and the discovery of a large number of reservoirs represented by the Mahu Depression, coarse-grained fan deposit reservoirs have attracted increasing attention from petroleum geologists worldwide (Krézsek et al., 2010; Pang et al., 2011; Zhao et al., 2016; Tang et al., 2019). Coarse-grained fan depositional systems mainly include alluvial fans and fan deltas, which are also potential reservoirs of hydrocarbon and coal (Prior, 1990; Gawthorpe and Leeder, 2000; Longhitano, 2008; Backert et al., 2010). According to statistics, the original geological reserves of fan deltas and alluvial fan reservoirs account for 11.8% of the current total (5.4% for the fan deltas and 6.4% for the alluvial fans) (Xu et al., 1998). Coarse-grained fans were usually developed in near-source areas and were sensitive to the response of piedmont tectonic activity, climate change, sediment supply rate, geomorphology, and base level rise/fall

Received November 30, 2022; accepted February 22, 2023

E-mail: lishunli@cugb.edu.cn

(DeCelles et al., 1991; Warrick et al., 2009; Waters et al., 2010; Gómez-Paccard et al., 2012; Fidolini et al., 2013; Tan et al., 2016; Zhu et al., 2016). Among these influencing factors, topographic slope change was an important condition for the deposition of coarse-grained fans. The response of fan sedimentation characteristics and their control mechanisms under different slope types and patterns has become a key aspect of current research (Yu et al., 2022). The topographic relief controlled the morphology of coarse-grained fans and their sediment characteristics. The coarse-grained fans were generally thick under steep topography and were dominated by gravel deposition. However, the coarse-grained fans were relatively thin-bedded with large areas under gentle topography and were commonly dominated by conglomerates interbedded with sandstones.

Sternberg (1875) established an exponential relationship between sedimentary grain size and transport distance. Subsequently, researchers have argued for and supported the relationship between sedimentary grain size and its transport distance based on his theory (Wan et al., 1987; Paola et al., 1992; Robinson and Slingerl, 1998; Hoey and Bluck, 1999; Attal and Lavé, 2009; Whittaker et al., 2011; Gale et al., 2019). For fan systems with a high rate of proximal deposition, changes in slopes were significant for sediment transport. Blair and McPherson (1994) investigated the Roaring River alluvial fan in Cassville, Missouri, USA, combining the morphological scale of the fan and surface slope descent contours with several profiles to characterize the topographic elevation differences and sediment grain size. That study concluded that the sediment grain size tended to become finer with the change in slope, the maximum grain size was usually developed under the slope break, and the sediment grain size also changed with the change in facies. Gao et al. (2022) found a relationship between sediment characteristics and the lake shoreline distance under several modern depositional systems. The gravel to sand transformation was close to the lake shoreline with sufficient sediment supply and/or under steep slopes. However, the gravel to sand transformation was far from the lake shoreline when the depositional slope gradients decreased.

The topographic slope for sediment transport was the key element that controlled depositional mechanisms, facies spreading, reservoir architectures and physical properties, which was a quantitative indicator of the degree of paleotopography and had an important influence on the surface material-energy migration and transformation, deposition pattern and the planar distribution of sand bodies. Therefore, topographic features and their slope gradients can characterize the variation in accommodation and influence the sediment supply (Harvey et al., 2005), which in turn controls the slope gradient and planform of various fans (Yu et al., 2013). Accurate calculation of paleotopographic slopes is recommended for analyzing sand spreading, internal architecture and the development of turbidites (Cao and Liu, 2007). However, due to the limitations of present-day technology and confusion surrounding the concept of paleotopographic slopes, the calculation of paleotopographic slopes has a certain bias (Yu et al., 2018).

A large number of fan-delta deposits at different scales were developed on the north-west margin of the Junggar Basin in the Triassic (Wei et al., 2005, 2007). In this paper, we described and interpreted the relationship between the sedimentary characteristics and slope patterns in the Upper Karamay Formation of Block 5 in the Karamay Oilfield, which is located on the north-west margin of the Junggar Basin, by using a large number of cores, wireline logs and seismic data.

The aims of this paper were (i) to describe the sedimentary facies associations of the Triassic fan-delta system on the north-west margin of the Junggar Basin; (ii) to build a sedimentary model of the fan – delta system under different slope patterns; (iii) to analyze the modern fan system; and (iv) to briefly discuss the flow transformation under different slope patterns.

## 2 Geological setting

As the second largest oil-bearing basin in north-west China, the Junggar Basin is bounded by the Karamaily Mountains, Tianshan Mountains and Zaiyre Mountains (Kang, 2011) (Fig. 1(a)). The study area is tectonically located in the Ke-Wu giant thrust fault zone on the north-west margin of the Junggar Basin. The Ke-Wu Fault is a hidden reverse-obscured fracture zone with NE striking (Fig. 1(b)) that was initially formed during the Hercynian tectonic movement stage and experienced several overthrusts during the Indo-China movement. The Triassic fault zone was accompanied by strong activity until the main rupture of the Early-Middle Jurassic fault zone, and the secondary rupture activity of the lower plate gradually weakened. The faults basically dip to the north-west in the profile, which is opposite to the tendency of the strata. The section is a high-angle retrograde fracture, steep at the top and gentle at the bottom.

The Upper Karamay Formation mainly consists of coarse-grained deposits dominated by pebbles to cobbles with granules, and it is in conformable contact with the underlying Lower Karamay Formation ($T_2k_1$) and the overlying Baijiantan Formation ($T_3b$). The Upper Karamay Formation is divided into four sections, including $T_2k_2^1$, $T_2k_2^2$, $T_2k_2^3$, and $T_2k_2^4$, from bottom to top. It was developed in a complete long-term cycle, representing the deposition from the transgressive to regressive phases of the fan delta.

The Ke-Wu Fault in the study area was a

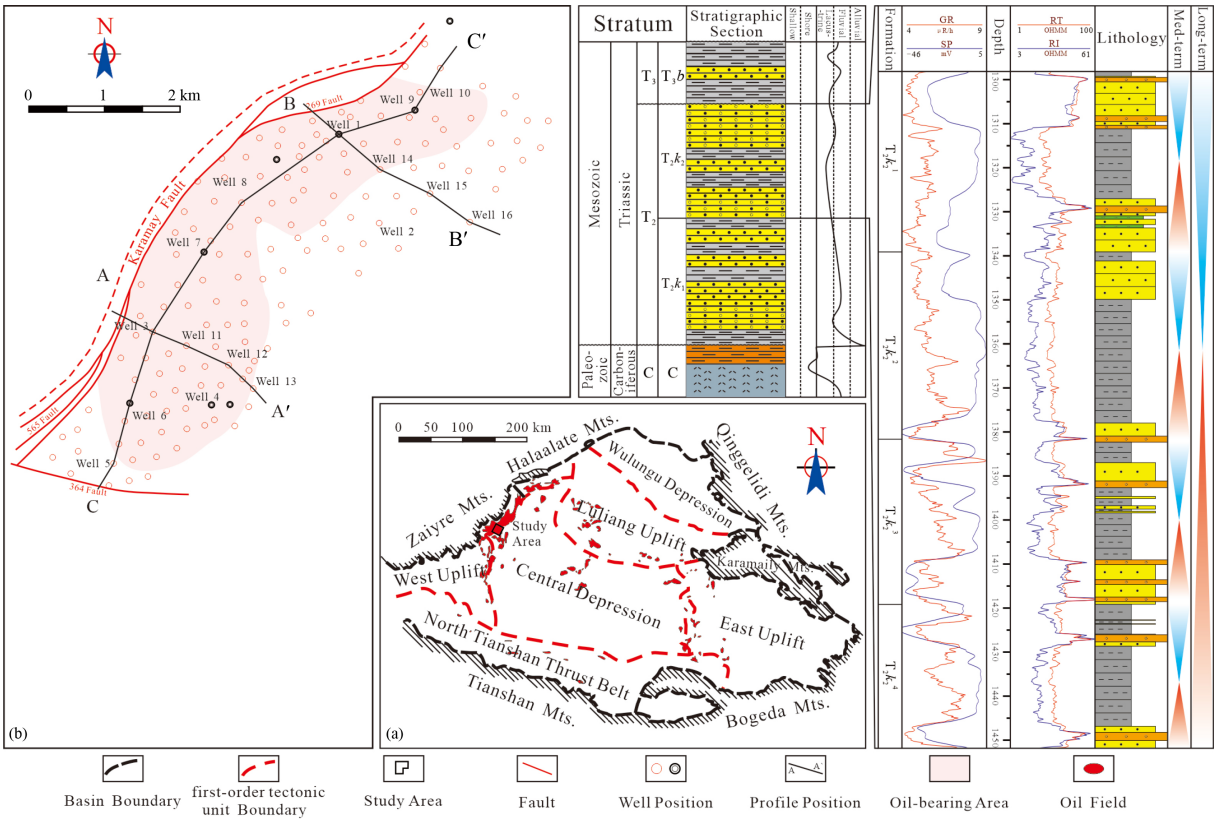


**Fig. 1** (a) The major structural units of the Junggar Basin. (b) Geological map, locations of the primary wells and stratigraphic column for the study area. Seismic lines A–A′ (Figs. 2(a) and 8), B–B′ (Figs. 2(b) and 9), C–C′ (Fig. 10) are indicated.

syndepositional fault with continuous activity during the depositional periods of the Upper Karamay Formation, which controlled the geomorphological features of the study area. Although the Ke-Wu Fault is a SE-dipping monocline, the slope patterns of the northern and southern geomorphologies are different. The relative slope changes in the northern and southern parts of the study area were compared and analyzed by measuring the stratigraphic reflection slope angles in the seismic profiles. The topography in the northern part of the study area was gentle and then steep, while the southern part was steep and then gentle. Nevertheless, the overall topographic characteristics of the study area were gentle to the north and steep to the south (Fig. 2).

The analysis of heavy mineral (tourmaline and zircon) data from four wells in the study area showed that there was a significant difference in the heavy mineral content ratio between the north (well 1 and well 2) and the south (well 3 and well 4) of the study area, with an overall tourmaline content of within 5% in the north and 5%–35% in the south and a zircon content of within 10% in the north and 10%–25% in the south (Fig. 3). The consistent pattern of heavy mineral content in the north and south also indicated the development of two sectors in the study area with two source systems at the same time. Moreover, the source rocks of these two fan deltas are dominated by medium-fine conglomerates, which are dominated by granites, and the clastic composition is mainly volcanic clastic rock (Gao, 2019). Therefore, we consider the two fan deltas developed in the study area to be two source systems with the same source rocks.

On the basis of previous studies, it has been concluded that the paleoclimate was warm and humid during the depositional periods of the Upper Karamay Formation (Huang et al., 2003; Xian et al., 2008; He et al., 2017; Huang et al., 2017).

## 3 Materials and methods

This study mainly includes measured core sections from 3 wells (total 124.3 m in thickness), well logs from 264 wells, and a 3D seismic survey covering 50 km$^2$. Core descriptions, including documentation of color, texture, compaction, sedimentary structure, and vertical distribution of grain size, were employed to identify sedimentary facies. Sedimentological analysis of the corresponding well logs was also used to identify stratigraphic surfaces and depositional environments. Wireline logs mainly include spontaneous potential (SP), gamma ray (GR), and resistivity logging (RT). The amplitude and geometry of logging curves have been used to interpret depositional elements.

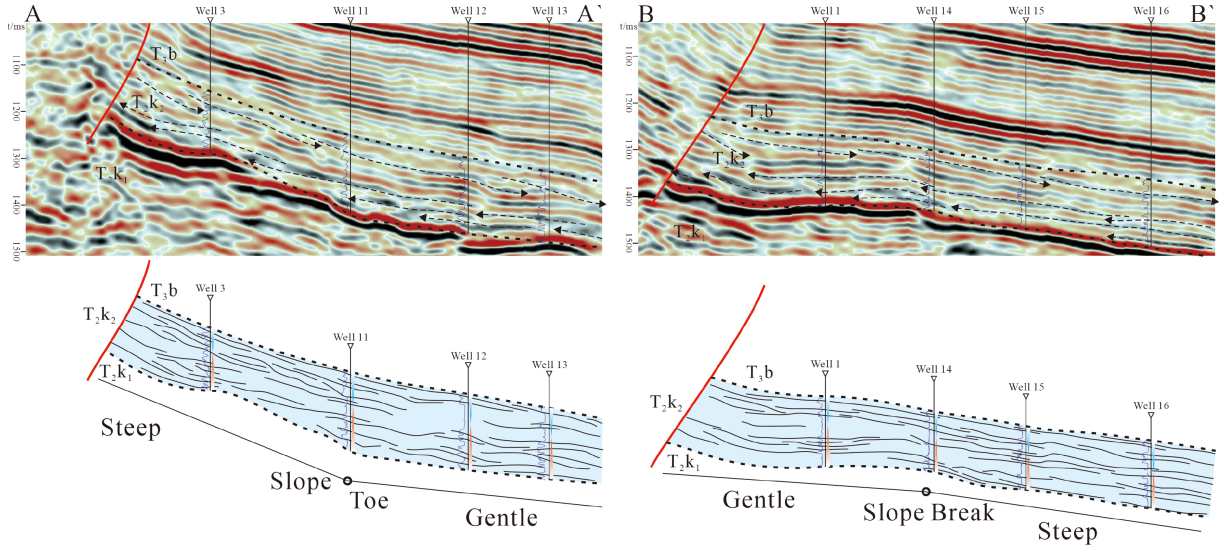


**Fig. 2** Seismic profiles of topographic slope differences between the north and south of the study area.

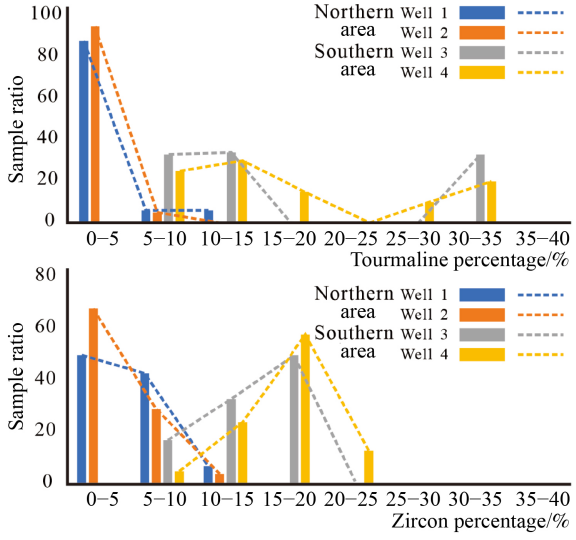


**Fig. 3** Heavy mineral compositions indicate that two sedimentary systems are developed in the north and south of the study area.

## 4 Results

### 4.1 Conglomeratic lithofacies

#### 4.1.1 Lithofacies categories

By observing and describing the lithology of the cores in the study area, the gravel deposits were petrographically classified according to the grain size, textural features and sedimentary structures of the conglomerates.

The conglomeratic facies in the study area include homograde, clast-supported conglomeratic lithofacies (Gcs); multigrade, clast-supported conglomeratic lithofacies (Gcm); gravelly matrix-supported conglomeratic lithofacies (Gmg); sandy matrix-supported conglomeratic lithofacies (Gms); imbricated conglomeratic lithofacies (Gi); graded bedding conglomeratic lithofacies (Gg); trough cross-bedded conglomeratic lithofacies (Gt); and planar cross-bedded conglomeratic lithofacies (Gp) (Fig. 4).

These conglomerate lithofacies can be classified into three flow regime categories, namely, debris flow, hyperconcentrated flow and traction current, which indicate different depositional processes (Tan et al., 2014, 2017).

The homograde, clast-supported conglomeratic lithofacies (Gcs) were coarse-grained deposits that were composed of gravels with moderate sorting and roundness and no obvious sedimentary structures. They were mostly found in granules in the study area, reflecting the gradual stabilization of hydrodynamic conditions, which was mostly deposited at the bottom of tractive currents. The conglomerates in the multigrade supported conglomeratic lithofacies (Gcm) were characterized by clast-supported, poorly sorted, moderately rounded pebbles and cobbles showing mostly blocky sequences, which were generally formed by debris flows. The gravelly matrix-supported conglomeratic lithofacies (Gmg) showed a sedimentary texture of granule matrix supporting cobbles and pebbles that were poorly sorted, moderately rounded, and had no obvious sedimentary structure. This facies was deposited in the initial section of the debris flows. The sandy matrix-supported conglomeratic lithofacies (Gms) exhibited poorly sorted and moderately rounded granules, and pebbles were supported by a fine-grained sandy matrix, which was mostly formed in debris flows with medium sediment concentrations. The imbricated conglomeratic lithofacies (Gi) were characterized by superimposed tabular cobbles and pebbles with poor sorting and moderate roundness, which represented the transition from debris flows to traction currents. The graded bedding conglomeratic lithofacies (Gg) were mainly composed of moderately sorted and rounded granules and pebbles showing fining-

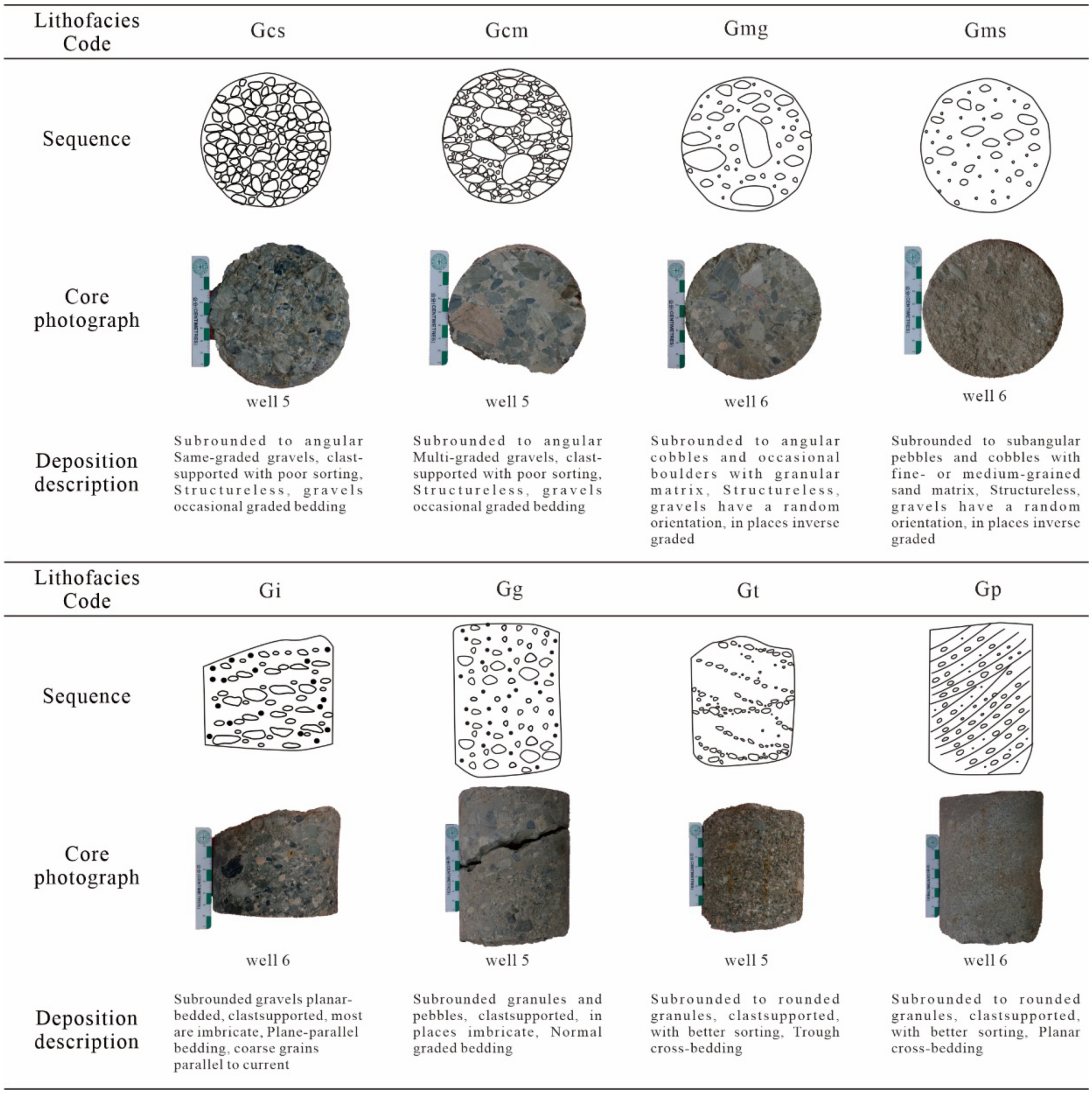


**Fig. 4** Categories of the Upper Karamay Formation lithofacies and genesis explanations. Lithofacies codes are modified from Miall (1977a). Gcs = homograde, clast-supported conglomeratic lithofacies; Gcm = Multi-grade clast-supported conglomerate; Gmg = Gravel-rich matrix-supported conglomerate; Gms = Sand-rich matrix-supported conglomerate; Gi = Imbricated planar-bedded conglomerate; Gg = Graded-bedded conglomerate; Gt = Trough cross-bedded conglomerate; Gp = Planar cross-bedded conglomerate.

upward sequences in the vertical direction, which indicated the flow transformation from debris flows to high-density turbidity currents. The trough cross-bedded conglomeratic lithofacies (Gt) consisted of stacked trough cross-stratifications with granules developed along the laminations, generally showing fining-upward sequences, which were developed by traction currents in channels. The planar cross-bedded conglomeratic lithofacies (Gp) were characterized by inclined stratifications with well-sorted and rounded granules, developing large-scale planar crossbeddings, which suggested lateral migration of gravelly macroforms under traction current action.

### 4.1.2 Lithofacies association

A single type of lithofacies reflected only depositional processes under certain hydrodynamics. The vertical association of lithofacies indicated the combined vertical characteristics of the sedimentary environments. Through detailed examination of cores, six kinds of lithofacies associations were identified, named FA-1 to FA-6 (Fig. 5). The components of the lithofacies associations were formed by different mechanisms, resulting in differences in their reservoir porosity, permeability characteristics, and oil production capacity.

FA-1, (Gmg→Gcm→Gcs), was dominated by pebbles and cobbles, consisting of Gmg, Gcm and Gcs from the bottom to the top, which showed a fining-upward grain size trend. This association exhibited a gradual decrease in sediment matrix content (clast- to matrix-supported) caused by the weakening and stabilization of hydrodynamic conditions, which was generally developed by

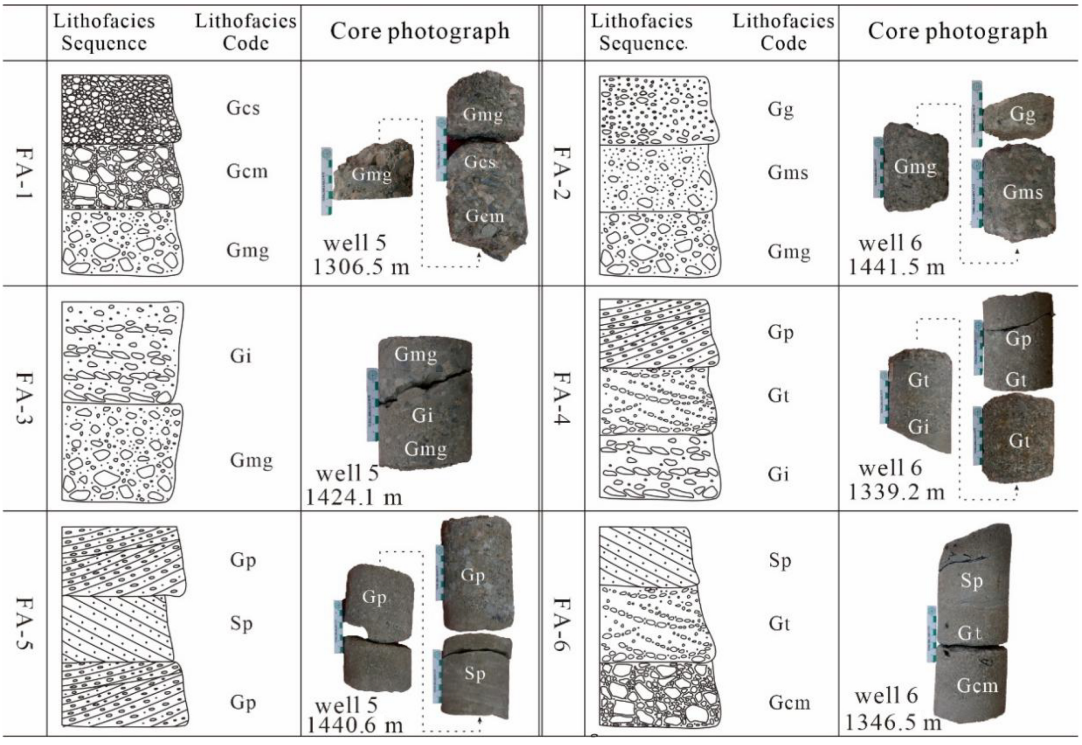


**Fig. 5** Classificataion of lithofacies associations in the Upper Karamay Formation.

highly concentrated debris flows in the proximal area of the fans.

FA-2, (Gmg→Gms→Gg), was dominated by clast- to sandy matrix-supported pebbles and cobbles, also showing fining-upward grain size features. The lithofacies of Gmg and Gcm still reflected debris flow deposition with relatively low clast concentrations.

FA-3, (Gmg→Gi), was dominated by clast-supported pebbles and cobbles with chaotic or imbricated sedimentary structures. This facies association generally exhibited a coarsening-upward sequence in the vertical direction, which suggested downstream progradation of the gravel macroforms formed by transitional flows between debris and traction (sheet floods).

FA-4, (Gi→Gt→Gp), was dominated by granules to pebbles with scour bases, imbricated structures and pervasive cross-stratification. The matrix content of the lithofacies gradually decreased upward, reflecting products from dominant traction currents with dilute debris flows.

FA-5, (Gp→Sp) was dominated by granules and sandy gravel with obvious fining-upward grain sizes. A slightly scoured base and relatively small-scale trough and planar cross-beddings were developed in this lithofacies association. The high content of sandy matrix indicates sedimentation of traction currents derived from depleted floods in the distal area.

FA-6, (Gcm→Gt→Sp), was mainly composed of granules and gravelly sandstone with massive, trough, planar cross-beddings. The multigrade clast-supported conglomerates and massive gravelly sandstone indicated sediment unloading at a relatively high rate.

Coarse-grained fan deltas developed in the study area. We considered FA-1 and FA-2 to be typical braided channels with differences mainly in grain size and matrix content. These two lithofacies associations corresponded to fluvial channel deposition within the fan delta plain under different slope gradients in the northern and southern fan deltas of the study area. We considered FA-3 to be a braided bar developed in the fan delta plain. We considered FA-4 and FA-5 to be braided distributary channels developed in the transitional part of the fan delta plain and fan delta front with significantly increased traction current deposition, respectively, with different grain sizes and traction current sequences at different slope gradients. We considered FA-6 to be a subaqueous channel developed in the fan delta front.

#### 4.1.3 Comparison of sedimentary characteristics between the northern and southern parts of the study area

Based on the description of the cores and the classification of the lithofacies associations, the lithology, sedimentary structures, and reflected sedimentary units were summarized and analyzed. The well 5 and well 6 were employed as examples to analyze the differences in sedimentary facies and their hydrodynamic conditions between the northern and southern parts of the study area. Due to the difference in the slope patterns of these two wells, there were significant differences in the depositional characteristics within the same sedimentary facies. Well 5 was mainly composed of coarse-grained sedime-

nts, such as pebbles and cobbles, medium- to coarse-grained sandstone, and gravelly sandstone, which constitute thick, multistory braided channels and braided bars of fan delta plain formed by debris flows without obvious sedimentary structures.

Well 6 was mainly composed of slightly finer sediments than those of well 5. It was mainly deposited by hyperconcentrated flow and traction currents. In the fan delta front, there were braided distributary channels, subaqueous distributary channels, distributary mouth bars and interdistributary bay facies consisting of granule or pebbly conglomerates and medium- or fine-grained sandstones with cross stratifications and granular laminations, which were slightly finer in grain size than the delta plain. The pro-fan delta was dominated by dark gray, fine-grained deposits, including siltstone and mudstone, which reflected stable, low energy hydrodynamic conditions (Fig. 6).

## 4.2 Sedimentary characteristics

### 4.2.1 Correlation of sedimentary facies

The spontaneous potential (SP) characteristics were used as a basis for identifying depositional facies in this study. By analyzing the amplitude, shape, top bottom contact relationship, smoothness and logging parameter response range, we established a log facies identification template for this study area, which represented 7 kinds of microfacies (Fig. 7).

The AA′ profile was located in the southern part of the study area (Fig. 1), with a NNW–SSE dip-orientation. This profile exhibited a slope pattern from steep to gentle. The fan delta plain and fan delta front were developed on this profile. The fan delta plain was dominated by braided channels and braided bars, and the fan delta front was dominated by subaqueous distributary channels and distributary mouth bars. In the sequence stratigraphy framework, $T_2k_2^4$ was developed in the lowstand system tract, which consisted of relatively thick-bedded sand bodies in the fan delta plain. The major thick sand body was formed close to the slope break and slope toe. $T_2k_2^3$ and $T_2k_2^2$ were mainly developed in the transgressive system tract with gradually rising lake level. The overall sedimentary characteristics showed retrogradation of the relatively thin-bedded sand bodies with well-developed muddy sedimentation. The scale of the fan delta plain gradually decreased, and the fan delta front reached the

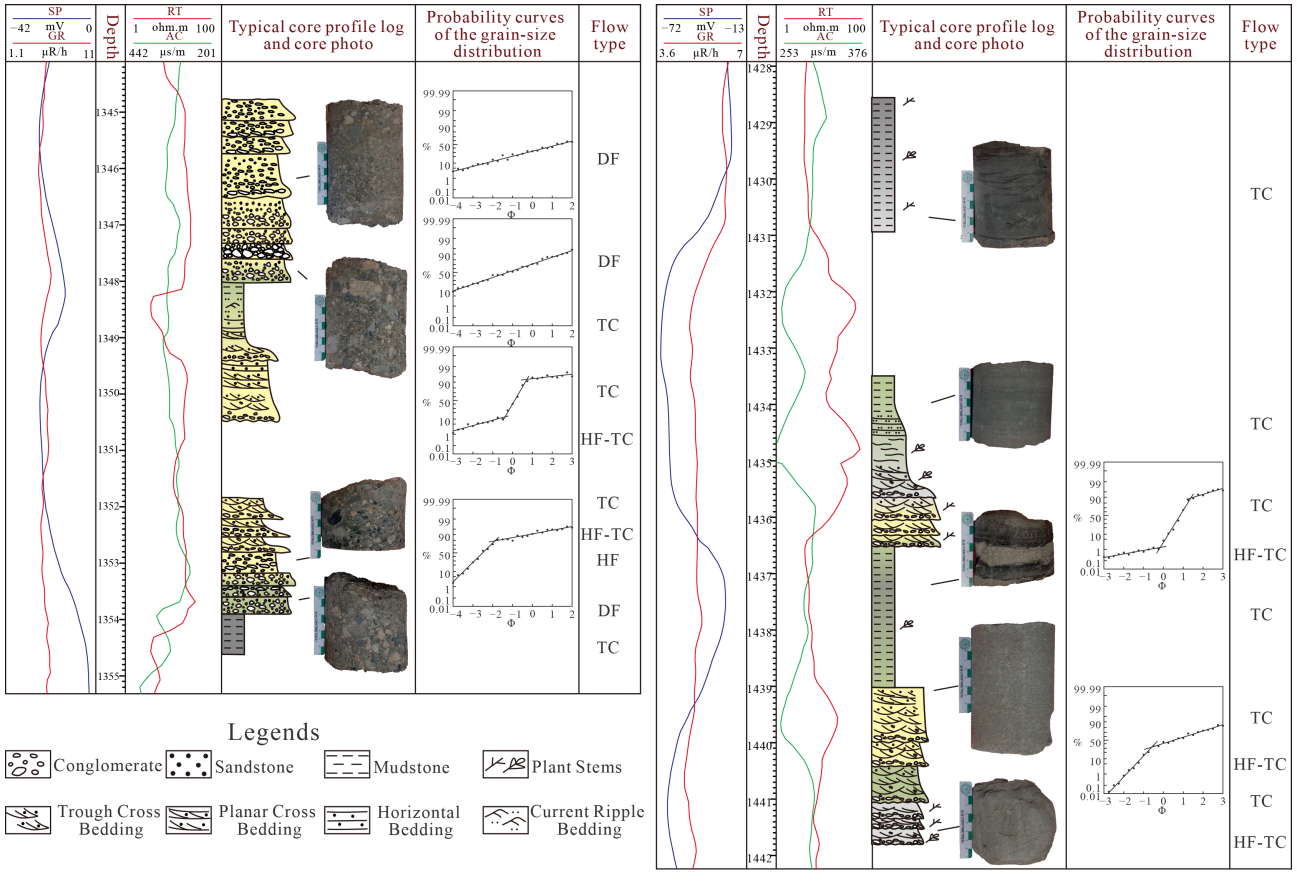


**Fig. 6** Typical vertical sequence for fan delta (left, Well 5) and braided river delta (right, Well 6) of the Upper Karamay Formation in study area, Junggar Basin. DF: Debris Flow; HF: Hyperconcentrated Flow; DF-HF: Debris-Hyperconcentrated Flow; TC: Tractive Current; HF-TC: Hyperconcentrated Flow - Tractive Current.

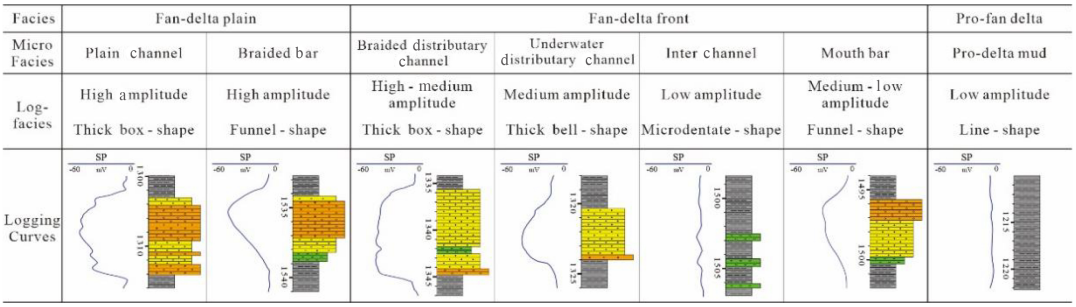


**Fig. 7** The Logging Curve characteristics of fan-delta facies.

maximum flood surface in late $T_2k_2^2$. $T_2k_2^1$ was formed in the highstand system tract when the lake level began to fall. The overall depositional characteristics showed progradation of thick-bedded sand bodies with increasing plain extension. In particular, the fan delta plain started to develop on a large scale with braided channels and braided bars deposited in the slope toe zone (Fig. 8).

The BB′ profile was located in the northern part of the study area (Fig. 1), with a NNW–SSE dip-orientation. This profile showed a slope pattern from gentle to steep. The fan delta plain and fan delta front were developed along the slope. The fan delta plain was dominated by braided channels and braided bars. The fan delta front was dominated by subaqueous distributary channels and distributary mouth bars. $T_2k_2^4$ was developed in the lowstand system tract. Sand bodies in the interval spread along the slope toe were relatively thinner than the equivalent in the south of the study area. $T_2k_2^2$ and $T_2k_2^3$ were in the transgressive system tract when the lake level began to gradually rise, developing retrogradation of thin-bedded sand bodies. The scale of the fan delta plain gradually decreased, but the fan delta front gradually expanded, which developed thick mudstone interbedded with medium- to thin-layered sandstone and conglomerates. Due to the rising lake level, the maximum flooding surface was reached at the end of the deposition period of $T_2k_2^2$. In this interval, the scale of fan delta development was small, and the sand bodies only spread along the slope toe zone. $T_2k_2^1$ was in the highstand system tract when the lake level began to fall. The overall depositional characteristics showed progradation of the fan delta. Thin-bedded sand bodies of the braided channels and bars were developed in the early stage, mainly spreading along the gentle slope and slope break zone. The sand bodies reached a maximum scale in the late stage, when the fan delta plain started to develop on a large scale with sets of thick-bedded sand bodies of braided channels and bars (Fig. 9).

The CC′ profile was located in the north-western part of the study area, which was the overall transversal profile

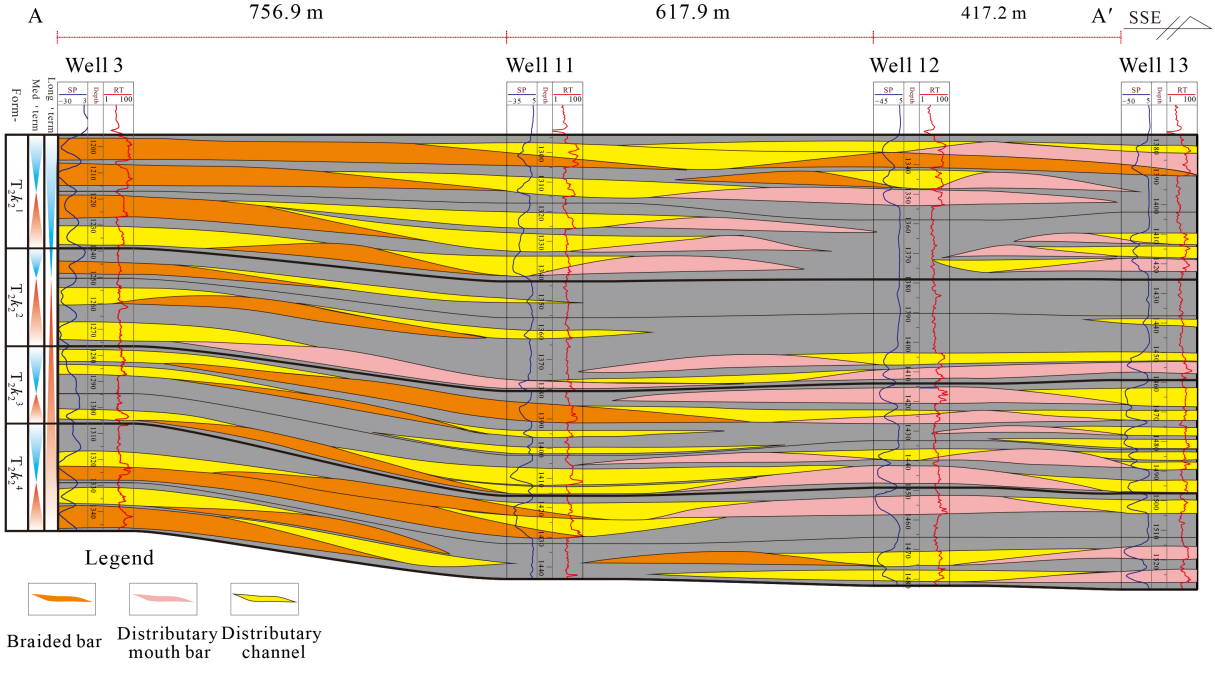


**Fig. 8** Sedimentary facies correlation in a dip-oriented section of the Upper Karamay depositional system in the south of study area, showing fan-delta plain deposits in proximal and fan-delta front deposits in distal.

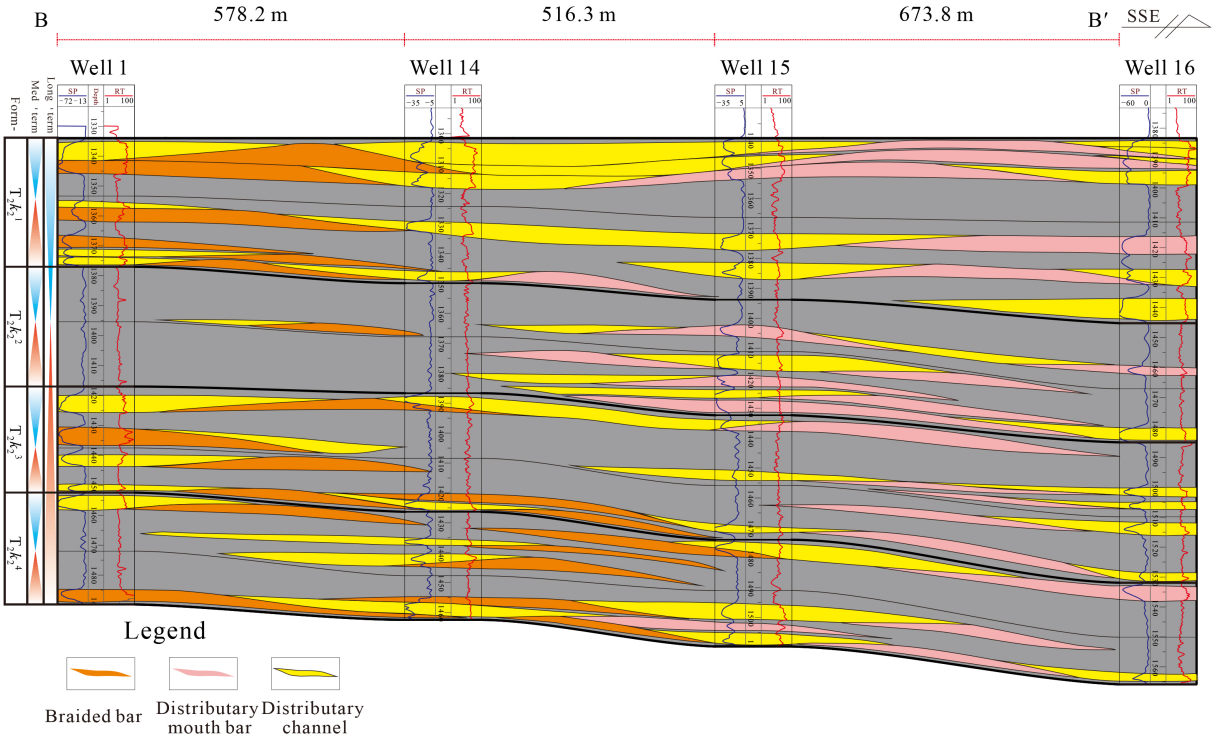


**Fig. 9** Sedimentary facies correlation in a dip-oriented section of the Upper Karamay depositional system in the north of study Area, which showing fan-delt plain deposits in proximal and fan-delta front deposits in distal.

striking in the SSW–NNE. This profile clearly showed that two subsidence centers developed in the study area from north to south, which correspond to the two fan delta systems developed in this area. The sand bodies in the south exhibited greater thickness and lateral extension than those in the north. $T_2k_2^2$ and $T_2k_2^3$ developed relatively small-scale sand bodies, while $T_2k_2^1$ had the largest scale (thickness and lateral extension) of sand bodies. The northern and southern boundaries of the fan deltas were between well 8 and well 1, respectively, in $T_2k_2^4$. The sand bodies, dominated by braided channels and bars, were mainly developed along the low area of the geomorphology. The thickness of sand bodies was greater in the south, while mud deposition was relatively lower in the north. The northern part was dominated by large sets of mudstone with thin-bedded conglomerates. Fan deltas in $T_2k_2^2$ and $T_2k_2^3$ gradually decreased in size due to lake level rise. Nevertheless, the northern fan delta shrank faster, resulting in thin-bedded, limited lateral extension of the sand bodies in the north. In the southern fan delta, the sand bodies were thick and dominated by frequent bar-channel superposition. The maximum flooding surface developed in the later period of $T_2k_2^2$ deposition, leading to small-scale fan deltas with thin-bedded sand bodies in this profile. The sand bodies were well developed in $T_2k_2^4$, which exhibited a large scale of the two fan deltas and a southward shift in the boundary between well 7 and well 8. The sand bodies were still dominated by frequent thick bar-channel transitions in the south and thin-bedded deposition in the north (Fig. 10).

#### 4.2.2 Distribution and evolution of the sedimentary systems

By studying seismic profiles, heavy mineral analysis and well correlations, we find that two fan deltas were obviously developed in the study area. The two fans were affected by differences in subsidence centers, slope patterns, and lake level changes. The scale of the southern fan delta varied relatively slowly and was dominated by more developed sand bodies and frequent bar-channel transitions. The scale of the northern fan varied relatively quickly and was dominated by relatively small-scale sand bodies and interdistributary channel deposits (Fig. 11).

Controlled by the difference in slope patterns under the steep-to-gentle slopes in the south, the coarse-grained delta showed an isometric fan shape in the plane view, which was mainly spread along the longitudinal axis. On the gentle-to-steep slopes in the north, the fan deltas were constrained in the plane view. After crossing the slope toe, the fan delta spread radially and rapidly in the lateral direction (Figs. 11 and 12).

The sedimentary evolution in the study area showed a complete long-term cycle of base level change from the bottom to the top of the formation, which consisted of LST, TST, and HST. In the LST ($T_2k_2^4$), the fan delta plain was confined near the slope toe zone, and the fan delta front was well developed, with a large front area and a small plain area. In the TST ($T_2k_2^2$ and $T_2k_2^3$), with the lake level rising, the scale of the fan delta was gradually restrained and shrank. The fan delta front gradually

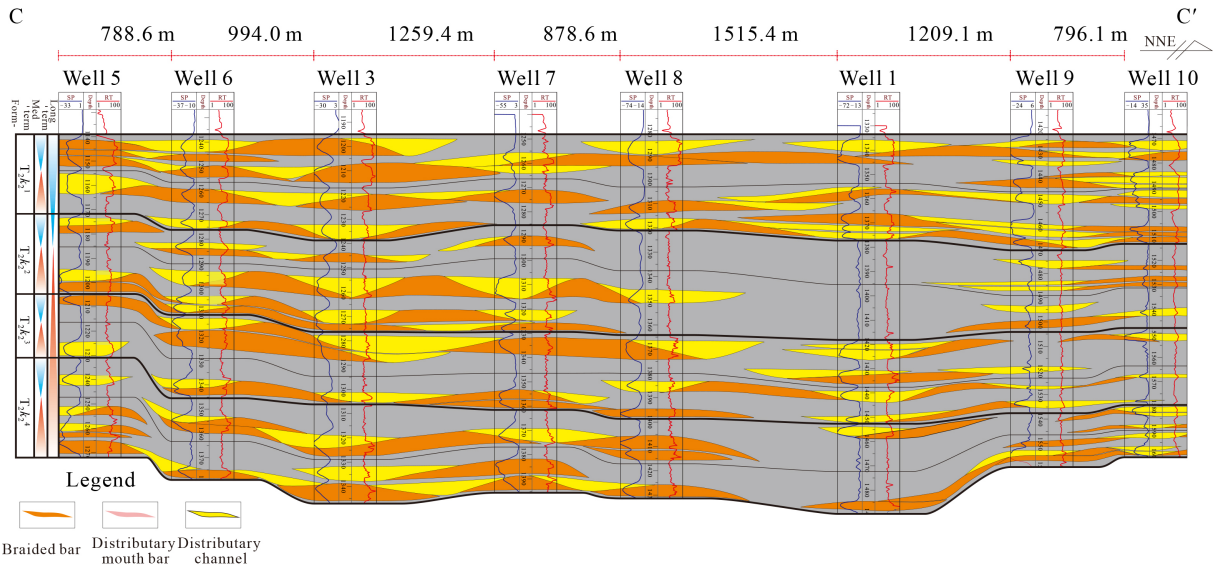


**Fig. 10** Sedimentary facies correlation in a dip-oriented section of the Upper Karamay depositional system in the south of study area, which showing fan-delta plain deposits in proximal and fan-delta front deposits in distal.

transformed into the pro-fan delta, with equal areas of plain and front. In the HST ($T_2k_2^1$), the scale (thickness and area) of the fan deltas gradually increased, and the intersection area of the two delta fans shifted southward. With the lake level fallling and the enhancement of sediment supply, the fan delta plain was well developed and had characteristics of a large area of plain and small area of front (Figs. 11 and 12).

#### 4.2.3 Depositional model of the fan deltas

In the Upper Karamay Formation, coarse-grained, clast- and matrix-supported, thick-bedded conglomerates were extensively developed with relatively poor sorting and roundness, which were deposited from debris flows, hyperconcentrated flows, and traction currents, reflecting strong hydrodynamic conditions. With the foundation of sedimentation analysis, fan delta systems were developed in the Upper Karamay Formation, showing different planform and sedimentary characteristics as a result of differences in slope patterns. Therefore, a combination model of the facies distribution and sedimentation background for the fan deltas on different slope patterns was established (Fig. 13). Consequently, the development characteristics of the fan deltas on different slope patterns can be summarized as elongate or equiaxial shapes on steep-to-gentle slopes, as convergent development occurs before the slope break and radially divergent development occurs after the slope toe on gentle-to-steep slopes.

## 5 Modern deposition analog

The Xiligou Fan Delta, which is a modern fan delta covering an area of approximately 35 km$^2$, is located 14 km south-west of Ulan County, Qinghai Province, China. Two major seasonally active channels have been developed on the fan delta. In this study, we conducted a detailed field study and trenching along the major active channel on the western side from the fan delta plain to the pro-fan delta. Combined with the geomorphic slopes and sedimentary characteristics, we observed that the coarsest gravel deposits (cobbles and boulders) were developed at the XLGH1 outlet, dominated by large sets of thick-bedded, structureless, sandy matrix-supported gravel. This result indicated significant debris flow deposition in the proximal area of the fan delta. The partially graded gravel beddings at XLGH2 became relatively finer (pebbles and cobbles), which indicated debris-hyperconcentrated flow deposition.

After crossing the slope break, the sedimentary slope gradients suddenly increased. The average grain size of the gravel sedimentation at XLGH3 increased again due to acceleration of transport energy. The homograde clast-supported, massive gravel sedimentation interbedded with sandy matrix-supported gravel indicated typical debris flow deposits developed at XLGH3. At XLGH4, with a continuous increase in transport distance, the sedimentary grain size gradually decrease. Graded beddings in the gravel interbedded with cross-stratified, gravelly coarse-grained sandy layers were developed.

At XLGH5, the deposits were mainly dominated by gravel with planar cross-beddings and graded beddings. The gravel on the scour surfaces was clearly oriented, suggesting traction current sedimentation at this position. On the gentle topography of XLGH6, massive and trough/planar cross-bedded sandy deposits were developed. However, laminated silty layers interbedded with muddy layers were observed at XLGH7. The sandy and muddy deposits at the fan delta front were products of significant traction currents and suspension deposition.

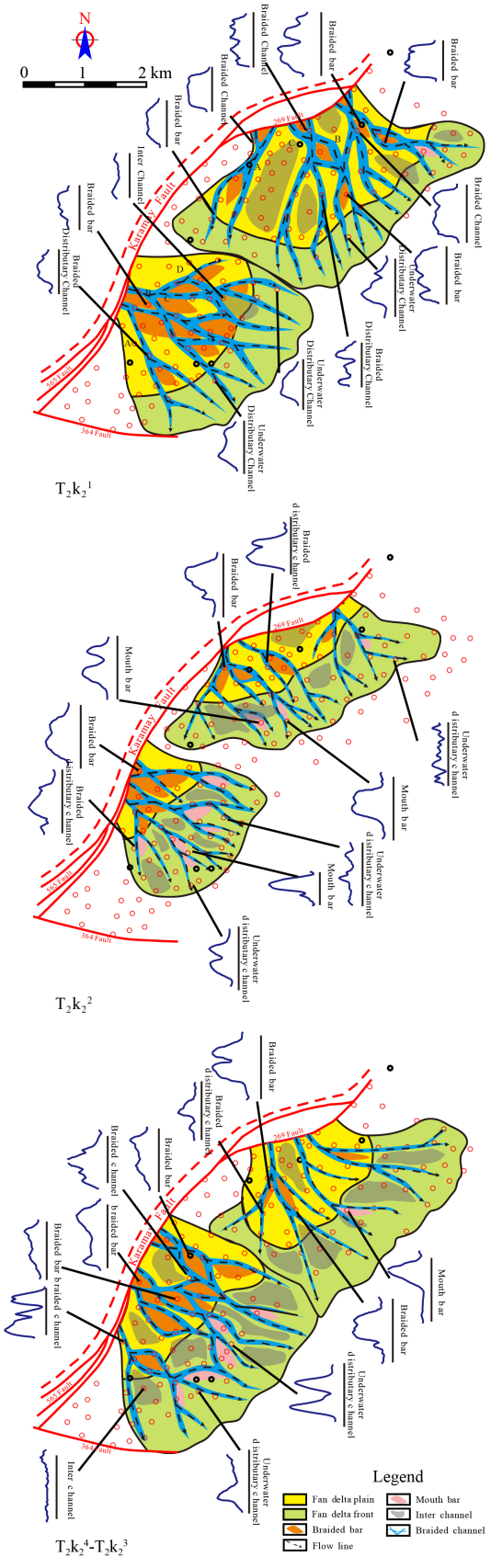


**Fig. 11** Distribution of sandstone and sedimentary microfacies in fan delta of the Upper Karamay Formation in study area.

This modern sedimentary analog indicated the control of the slope pattern on sedimentary hydrodynamics, which ultimately influenced the sedimentary characteristics of the fan delta on the gentle-to-steep slopes (Fig. 14).

## 6 Discussion

### 6.1 Relationship between flow regimes and transport distance

Since the classical experimental studies of Gilbert and Murphy (1914), it has been known that high velocity flows can carry a given amount of sediment at lower slope gradients. Miall (1977b) found slope to be a dependent variable when observing natural alluvium and specifically emphasized the importance of flow regime in determining the slope of alluvial fans. Differences in sedimentation and the main controlling factors in different slope backgrounds of typical alluvial fans and fan deltas around the world have been clarified by statistically analyzing 49 observations that were grouped by flow dominance (Boothroyd and Ashley, 1975; Stanistreet and McCarthy, 1993; Blair, 1999a, 1999b, 2000; Krapf et al., 2005; Shukla, 2009; Chakraborty et al., 2010; Gao et al., 2020). The results indicated that traction currents and hyperconcentrated flows showed a significant slope distinction (approximately 2°), while there was no significant slope distinction point for the conversion between hyperconcentrated flows and debris flows. However, in general, as the slope gradient increased, the hyperconcentrated flows converted to debris flows (greater than 8°–10°). In brief, there was a significant relationship between slope gradients and flow regimes, and as the slope increased, the sediment converted from traction current to hyperconcentrated and debris flow.

### 6.2 Flow transformation under different slope patterns

The two fan deltas developed in the study area were similar in terms of sediment supply, and the factors that caused the significant differences in sedimentary characteristics mainly depended on the differences in slope patterns. Flow regimes on different slope patterns showed obvious differentiation (Fig. 15(b)), especially the clear boundary between traction currents and hyperconcentrated flows. The transformation between these flows required significant slope change. However, the range of slope gradients for hyperconcentrated and debris flows exhibited overlap (7°–13°), which also indicated that the direct transformation between these flows was more frequent. In other words, a slight change in the slope gradient may cause flow transformation.

After idealizing and modeling the slope patterns of both fan deltas, they can be divided into two patterns: steep-to-gentle and gentle-to-steep (Fig. 16).

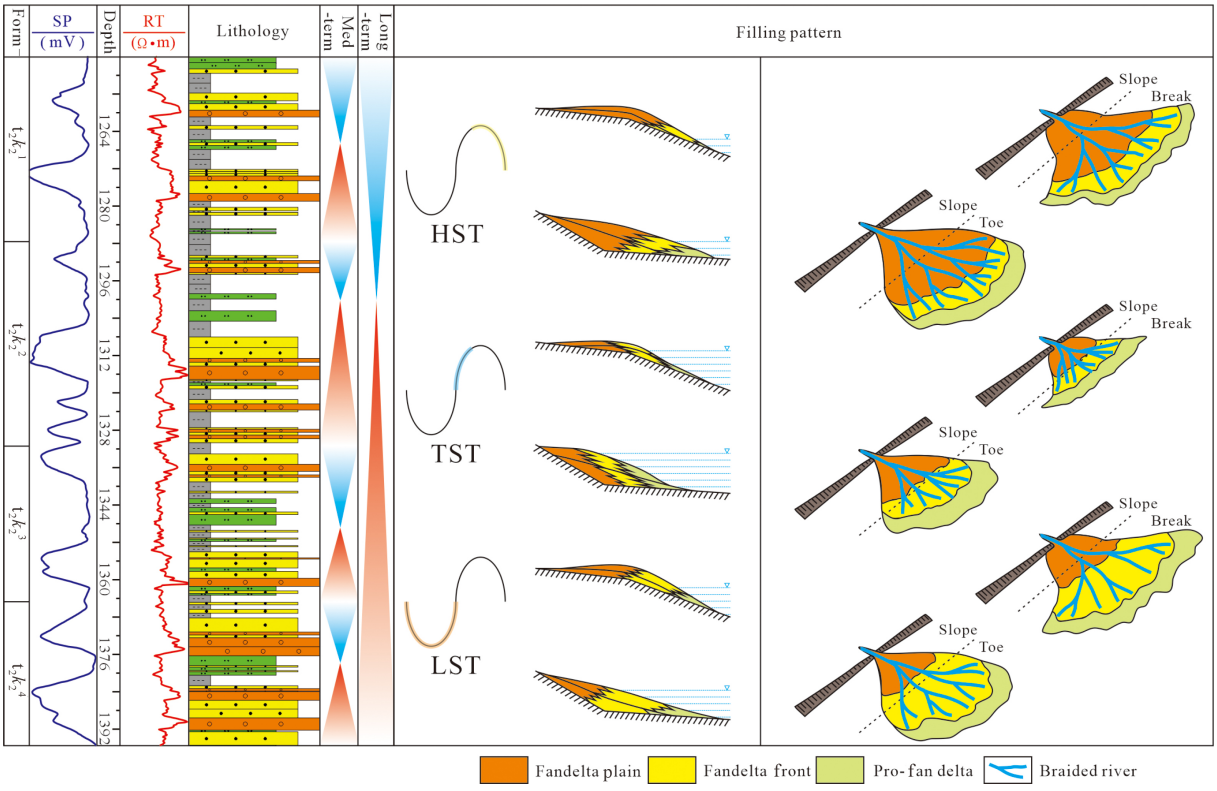


**Fig. 12** The characteristics of sedimentary evolution with different slope-pattern in the study area.

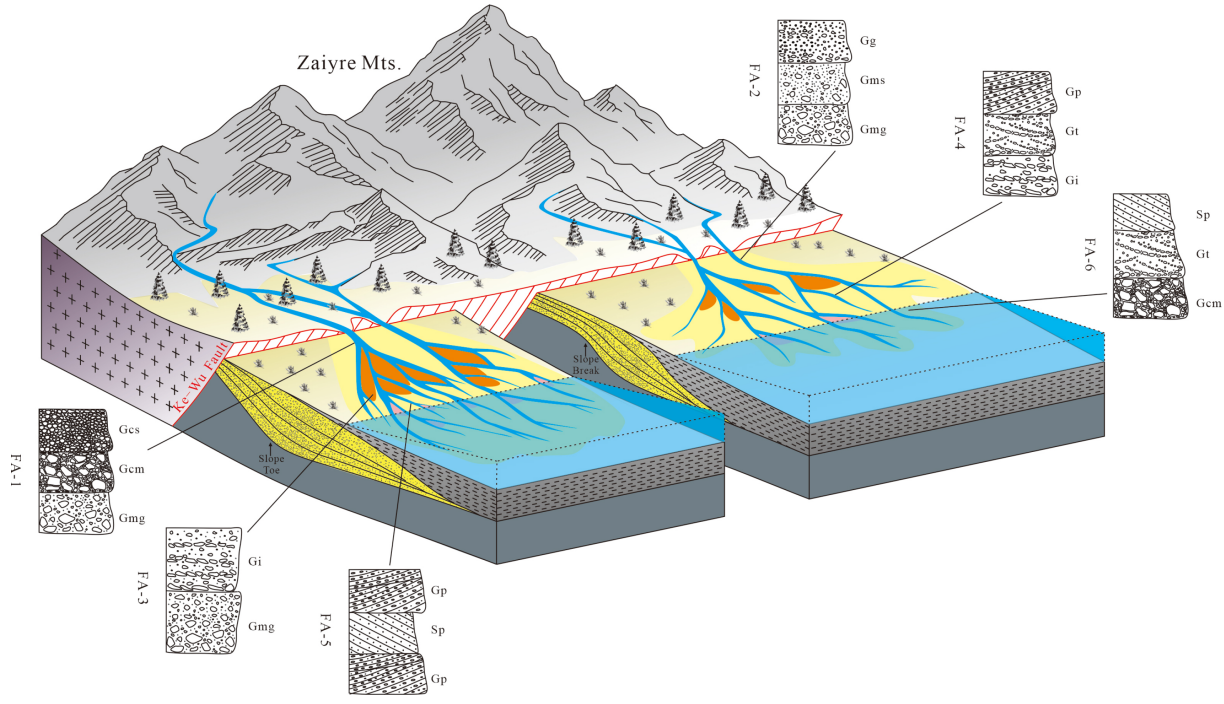


**Fig. 13** Distribution pattern of the fan deltas in different slope patterns.

### 6.2.1 Steep-to-gentle slopes

Sediments were transported into the basin from the feeder channels, maintaining a large amount of kinetic energy on the steep slope section. With adequate sediment supply, deposition occurred along the channel, developing multi-phase, thick debris flow deposition. The hydrodynamic force gradually weakened with increasing transport distance, which still mainly developed debris flow deposition with finer particles and enhanced textural maturity.

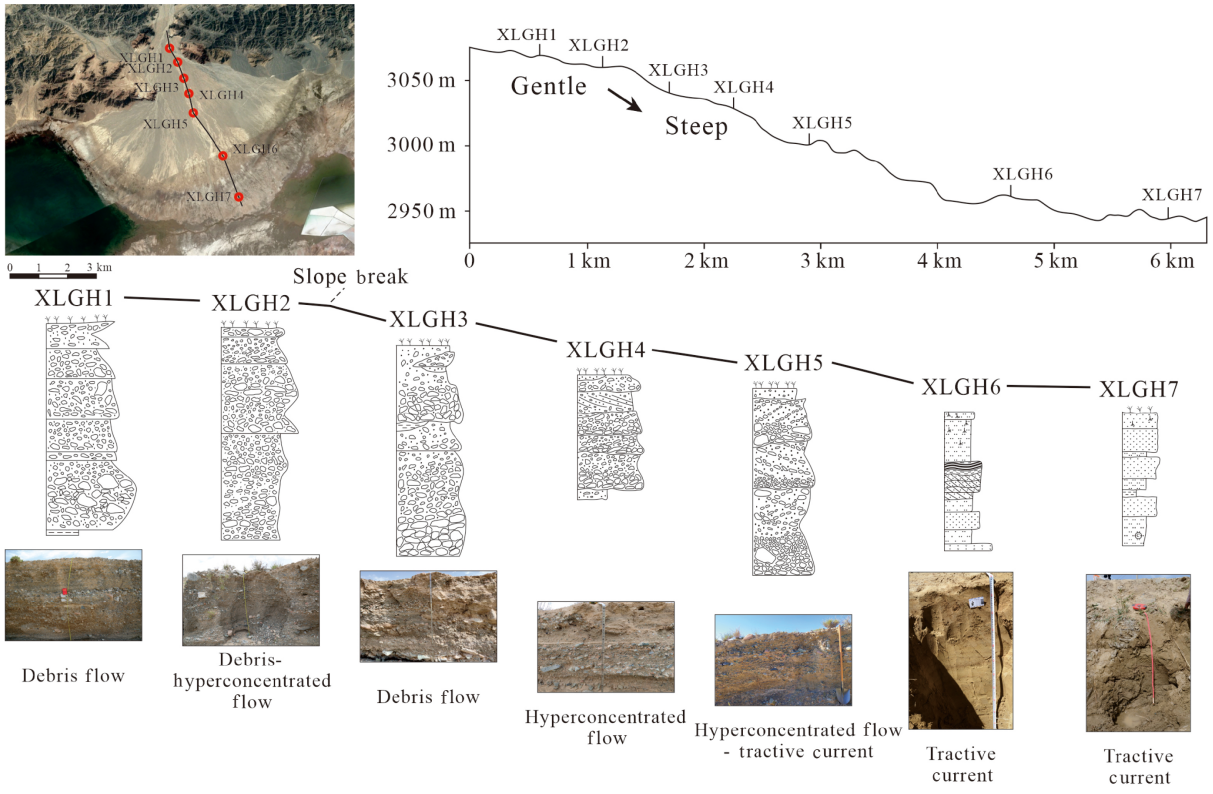


**Fig. 14** Modern fan delta deposition in Xiligou Lake, Qinhai, China.

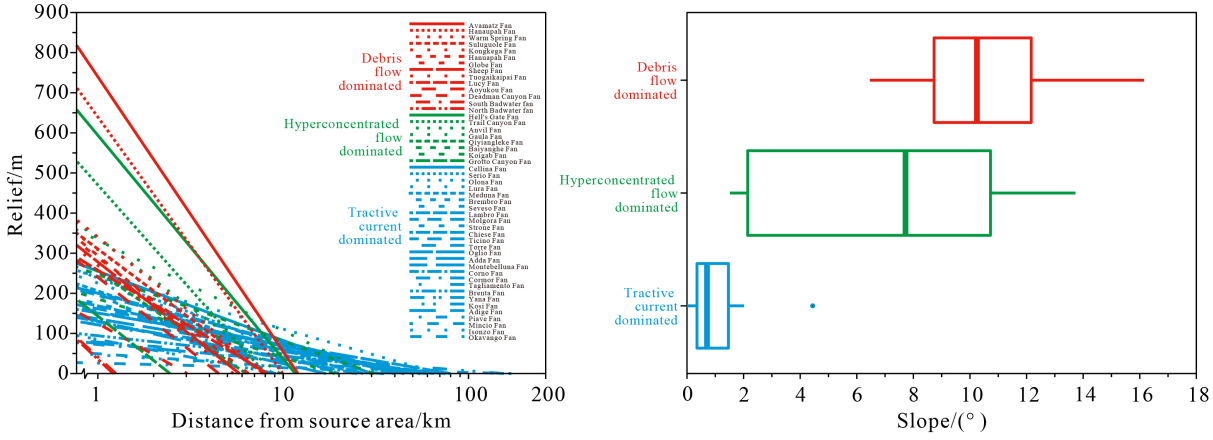


**Fig. 15** (a) Comparison of the gradients of the modern fans and fan deltas around the world, which are dominated by different primary processes. (b) The boxplot of the gradients and primary processes.

After crossing the slope toe, the slope pattern changed from steep to gentle, and the resistance of sediment transport increased rapidly. With hydrodynamic conditions and kinetic energy damping, sediments radiated along the slope toe zone and expanded rapidly. At the distal part of the slope, hyperconcentrated flows to traction currents were finally dominant in the fan delta front deposition.

### 6.2.2 Gentle to steep slopes

Sediments were transported into the basin from the feeder channel under a gentle slope with high flow resistance. Although the hydrodynamic force was strong and the sediment supply was adequate, a thick deposition could not be formed due to the lack of unloading space, developing debris-hyperconcentrated flow deposition. After crossing the slope break, the slope pattern changed from gentle to steep, and the unloading space and kinetic energy increased rapidly. Meanwhile, the flow of deposition converted from a debris hyperconcentrated flow to a debris flow, which developed a thick layer and spread radially. At the distal part of the slope, hyperconcentrated flows to traction currents were finally dominant in the fan delta front deposition.

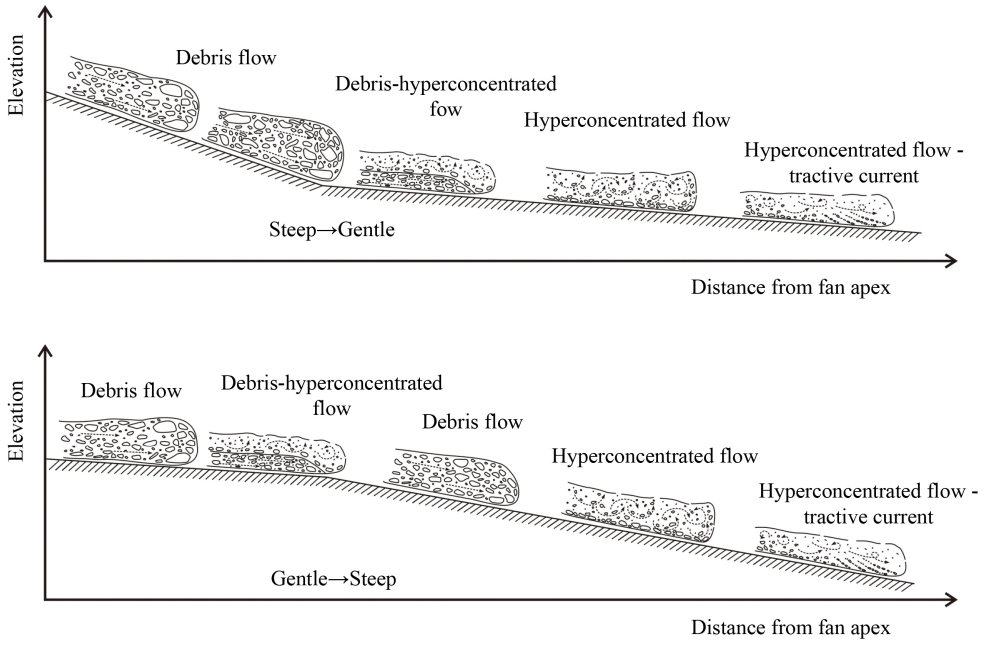


**Fig. 16** Sedimentogenesis and flow transformation under differential slope-patterns.

## 7 Conclusions

The following are the conclusions of this study.

1) Based on observations and descriptions of the fan-delta system of the Upper Karamay Formation on the north-west margin of the Junggar Basin, 8 types of conglomerate lithofacies and 6 types of lithofacies associations were identified.

2) Based on the seismic and well log data, different slope patterns between the north and south parts of the study area were identified, i.e., the southern part had a steep to gentle slope, while the northern part had a gentle to steep slope. According to the analysis of heavy minerals, two source systems of fan deltas developed in the study area from north to south.

3) The difference in slope pattern between the north and south influenced the sedimentary characteristics and vertical sequence of the fan deltas. The scale of sand body development was also influenced by this, with the sand body in the south being more developed and showing frequent bar-channel conversion and channel downcutting, whereas the sand body in the north was relatively thinly developed and dominated by isolated channels and less bar-channel conversion. The sand body spread mainly along the toe of the slope, and its planar spread was also influenced by the change in slope pattern. The southern part showed an obvious equiaxed fan shape. The northern part was relatively confined in the gentle slope section and spread radially after crossing the slope break, and its fan extension distance was shorter than that of the southern part.

4) Combined with the study of the fan delta of the Upper Karamay Formation and the modern fan delta of Lake Xiligou, it is clear that the difference in slope pattern had a certain control on the sedimentary characteristics and planar spreading characteristics of fan deltas and on the change in their dominant flow.

5) By statistically analyzing the relationship between the transport distance and elevation of 49 typical alluvial fans and fan deltas with different dominant factors worldwide, the control of slope pattern on the deposition of coarse-grained fans was clarified. A model of the transformation of the sedimentary characteristics under the different slope patterns was established.

**Acknowledgment** This study was supported by the National Natural Science Foundation of China (Grant No. 42272124), the Fundamental Research Funds for the Central Universities (No. 2-9-2019-100), the National Major Research Program Science and Technology of China (No. 2017ZX05001-002), and the Key laboratory of marine reservoir evolution and hydrocarbon enrichment mechanism, Ministry of Education. We are grateful to the School of Energy Resources, China University of Geosciences (Beijing).

**Conflicts of Interest** The authors declare no conflict of interest.

## References

Attal M, Lavé J (2009). Pebble abrasion during fluvial transport: experimental results and implications for the evolution of the sediment load along rivers. J Geophys Res Earth Surf, 114: F04023

Backert N, Ford M, Malartre F (2010). Architecture and sedimentology of the Kerinitis Gilbert-type fan delta, Corinth Rift, Greece. Sedimentology, 57(2): 543–586

Blair T C (1999a). Sedimentology of the debris-flowdominated Warm Spring Canyon alluvial fan, Death Valley, California.

Sedimentology, 46(5): 941–965

Blair T C (1999b). Sedimentary processes and facies of the waterlaid Anvil Spring Canyon alluvial fan, Death Valley, California. Sedimentology, 46(5): 913–940

Blair T C (2000). Sedimentology and progressive tectonic unconformities of the sheetflood-dominated Hell's Gate alluvial fan, Death Valley, California. Sediment Geol, 132(3–4): 233–262

Blair T C, McPherson J G (1994). Alluvial fan processes and forms. In: Abrahams A D, Parsons A J, eds. Geomorphology of Desert Environments. Dordrecht: Springer Netherlands

Boothroyd J C, Ashley G M (1975). Process, bar morphology and sedimentary structures on braided outwash fans, North-eastern Gulf of Alaska. In: Jopling A V, McDonald B C, eds. Glaciofluvial and Glaciolacustrine Sedimentation. Soc Econ Paleontol Mineral Spec Publ, 23: 193–222

Cao Y, Liu H (2007). Discussion on the relationship between distribution of fluxoturbidite and depositional slope of delta in lacustrine basin. Geol Rev, 53(4): 454–459

Chakraborty T, Kar R, Ghosh P, Basu S (2010). Kosi megafan: historical records, geomorphology and the recent avulsion of the Kosi River. Quat Int, 227(2): 143–160

DeCelles P G, Gray M, Ridgway K, Cole R, Pivnik D, Pequera N, Srivastava P (1991). Controls on synorogenic alluvial-fan architecture, Beartooth Conglomerate (Palaeocene), Wyoming and Montana. Sedimentology, 38(4): 567–590

Fidolini F, Ghinassi M, Aldinucci M, Billi P, Boaga J, Deiana R, Brivio L (2013). Fault-sourced alluvial fans and their interaction with axial fluvial drainage: an example from the Plio-Pleistocene Upper Valdarno Basin (Tuscany, Italy). Sediment Geol, 289: 19–39

Gale S, Ibrahim Z, Lal J, Sicinilawa U (2019). Downstream fining in a megaclast-dominated fluvial system: the Sabeto River of western Viti Levu, Fiji. Geomorphology, 330: 151–162

Gao C, Ji Y, Wu C, Jin J, Ren Y, Yang Z, Liu D, Huan Z, Duan X, Zhou Y (2020). Facies and depositional model of alluvial fan dominated by episodic flood events in arid conditions: an example from the Quaternary Poplar Fan, north-western China. Sedimentology, 67(4): 1750–1796

Gao M (2019). Study on the Reservoir Architecture and Macroscopic Heterogeneities of the the Upper Karamay Formation in the Wu1 Block, Karamay Oilfield. Beijing: China University of Geosciences (Beijing) (in Chinese)

Gao Z, Shi Y, Feng J, Zhou C, Luo Z (2022). Lithofacies paleogeography restoration and its significance of Jurassic to Lower Cretaceous in southern margin of Junggar Basin, NW China. Petroleum Exploration and Development, 49(1): 78–93

Gawthorpe R L, Leeder M R (2000). Tectono-sedimentary evolution of active extensional basin. Basin Res, 12(3–4): 195–218

Gilbert G K, Murphy E C (1914). The transportation of debris by running water. US Government Printing Office

Gómez-Paccard M, López-Blanco M, Costa E, Garcés M, Beamud E, Larrasoaña J C (2012). Tectonic and climatic controls on the sequential arrangement of an alluvial fan/fan-delta complex (Montserrat, Eocene, Ebro Basin, NE Spain). Basin Res, 24(4): 437–455

Harvey A M, Mather A E, Stokes M (2005). Alluvial fans: geomorphology, sedimentology, dynamics — introduction. A review of alluvial-fan research. Spec Publ Geol Soc Lond, 251(1): 1–7

He M, Zhang L, Liu Y, Li T, Zhang W (2017). Sedimentary system and environment research on the Triassic strata in northwest Junggar Basin. Geol Bull China, 36(6): 1032–1042

Hoey T B, Bluck B J (1999). Identifying the controls over downstream fining of river gravels. J Sediment Res, 69(1): 40–50

Huang K, Zhan J Z, Zou Y, Wang Z, Zhou C, Xiao J (2003). Sedimentary environments and paleoclimate of the Triassic and Jurassic in Kuqa river area, Xinjiang. J Paleogeogr, 5(2): 197–208

Huang Y, Zhang C, Zhu R, Yi X, Qu J, Tang Y (2017). Palaeoclimatology, provenance and tectonic setting during late Permian to middle Triassic in Mahu sag, Junggar Basin. China Earth Sci, 42(10): 1736–1749

Kang Z (2011). Evolution of Paleozoic sedimentation of the Junggar Basin. J Geomechanics, 17(02): 158–174

Krapf C B E, Stanistreet I G, Stollhofen H (2005). Morphology and fluvio-aeolian interaction of the tropical latitude, ephemeral braided-river dominated Koigab Fan, north-west Namibia. Spec Publ int Assoc Sediment, 35: 99–120

Krézsek C, Filipescu S, Silye L, Maţenco L, Doust H (2010). Miocene facies associations and sedimentary evolution of the Southern Transylvanian Basin (Romania): implications for hydrocarbon exploration. Mar Pet Geol, 27(1): 191–214

Longhitano S G (2008). Sedimentary facies and sequence stratigraphy of coarse-grained Gilbert-type deltas within the Pliocene thrust-top Potenza Basin (Southern Apennines, Italy). Sediment Geol, 210(3–4): 87–110

Miall A D (1977a). A review of the braided-river depositional environment. Earth Sci Rev, 13(1): 1–62

Miall A D (1977b). Fluvial sedimentology. Canadian Society of Petroleum Geologists, 123: 128

Pang X, Li P, Chen D, Zhang S, Zhang J, Yu Y (2011). Characteristics and basic model of facies controlling oil and gas in continental fault basin. J Palaeogeogr, 13(1): 55–74

Paola C, Heller P L, Angevine C L (1992). The large-scale dynamics of grain-size variation in alluvial basins, 1: Theory. Basin Res, 4(2): 73–90

Prior D B (1990). Fan-delta facies associations in late Neogene and Quaternary basin of southeastern Spain. In: Colella A, Prior D B, eds. Coarse-Grained Deltas International Association of Sedimentologists. Special Publications, 10: 91–112

Robinson R A, Slingerl R L (1998). Grain-size trends, basin subsidence and sediment supply in the Campanian Castlegate Sandstone and equivalent conglomerates of central Utah. Basin Res, 10(1): 109–127

Shukla U K (2009). Sedimentation model of graveldominated alluvial piedmont fan, Ganga Plain, India. Int J Earth Sci, 98(2): 443–459

Stanistreet I G, McCarthy T S (1993). The Okavango Fan and the classification of subaerial fan systems. Sediment Geol, 85(1–4): 115–133

Sternberg H (1875). Investigation of longitudinal and transverse profiles of bedload fluvial systems. J Construction, 25: 483–506 (in German)

Tan C, Yu X, Li S, Shan X, Chen B (2016). Sedimentology and stratigraphic evolution of the fan delta at the Badaowan formation (Lower Jurassic), Southern Junggar Basin, Northwest China. Arab J Geosci, 9(2): 12

Tan C, Yu X, Liu B, Qu J, Zhang L, Huang D (2017). Conglomerate categories in coarse-grained deltas and their controls on hydrocarbon reservoir distribution: a case study of the Triassic Baikouquan Formation, Mahu Depression, NW China. Petrol Geosci, 23(4): 403–414

Tan C, Yu X, Qu J, Wang Z, Li X, Gao Z (2014). Complicated conglomerate lithofacies and their effects on hydrocarbons. Petrol Sci Technol, 32(22): 2746–2754

Tang Y, Guo W, Wang X, Bao H, Wu H (2019). A new breakthrough in exploration of large conglomerate oil province in Mahu Sag and its implications. Xinjiang Petrol Geol, 40(2): 1

Wan J, Ma L, Zhou Z, Zhang Y (1987). Some problems in the study of sedimentary facies of deformed basin. Oil & Gas Geol, 8(4): 448–453

Warrick J A, Rubin D M, Ruggiero P, Harney J N, Draut A E, Buscombe D (2009). Cobble Cam: grain-size measurements of sand to boulder from digital photographs and autocorrelation analyses. Earth Surface Processes Landforms, 34(13): 1811–1821

Waters J, Jones S, Armstrong H (2010). Climatic controls on late Pleistocene alluvial fans, Cyprus. Geomorphology, 115(3–4): 228–251

Wei Y, Hu S, Lei Z, He D, Zhang L, Xu S (2005). Sedimentary response to Triassic-Jurassic thrust faulting in the foreland thrust belt of the northwestern Junggar Basin. Earth Sci Front, 12(4): 423–437

Wei Y, Li D, Hu S, Lei Z, He D (2007). Fans sedimentation and exploration direction of fan hydrocarbon reservoirs in foreland thrust belt of the northwestern Junggar Basin. Acta Geoscientica Sinica, 1: 62–71

Whittaker A C, Duller R A, Springett J, Smithells R A, Whitchurch A L, Allen P A (2011). Decoding downstream trends in stratigraphic grain size as a function of tectonic subsidence and sediment supply. Geol Soc America Bull, 123(7–8): 1363–1382

Xian B, Xu H, Jin Z, Wang C, Lu Y, Huang L (2008). Sequence stratigraphy and subtle reservoir exploration of Triassic system in northwestern margin of Junggar basin. Geol J China U, 14(2): 139

Xu A, Mu L, Qiu Y (1998). Distribution pattern of OOIP and remaining mobile oil in different types of sedimentary reservoir of China. Petrol Explor Develop, 25(5): 57–60,5–6,12–13 (in Chinese)

Yu X, Li S, Li S (2013). Texture-genetic classifications and mapping methods for deltaic deposits. Acta Sediment Sin, 31(5): 782–797

Yu X, Li S, Sun H (2022). Coupling effect of “mass-slope” from source to sink in clastic rock deposition. J Palaeogeogr, 24(06): 1037–1057

Yu X, Li S, Tan C (2018). Coarse-grained deposits and their reservoir characterizations: a look back to see forward and hot issues. J Palaeogeogr, 20(5): 713–736

Zhao Z, Xu S, Jiang X, Lin C, Cheng H, Cui J, Jia L (2016). Deep strata geologic structure and tight sandy conglomerate gas exploration in Songliao Basin, East China. Petrol Explor Develop, 43(1): 13–25

Zhu X, Zhong D, Yuan X, Zhang H, Zhu S, Sun H, Gao Z, Xian B (2016). Development of sedimentary geology of petroliferous basins in China. Petrol Explor Develop, 43(5): 820–829